Understanding Frequency Response of Induction Motor Winding through Electromagnetic Wave Equations

Hormaz Amrolia[1], *Santosh C. Vora*[2], *K. P. Badgujar*[1]

[1]L.D. College of Engineering, Electrical Engineering Department, Gujarat Technological University, Ahmedabad, India
[2]Institute of Technology, Electrical Engineering Department, Nirma University, Ahmedabad, India

hormaz.amrolia@gmail.com, santoshvora@yahoo.com, dr.ketanbadgujar@gmail.com

DOI: 10.15598/aeee.v21i3.5029

Article history: Received Jan 10, 2023; Revised Jun 21, 2023; Accepted Jul 10, 2023; Published Sep 30, 2023.

Abstract. *Frequency response analysis offers an insight about the integrity of machine windings, when employed as a tool for condition monitoring. To ensure that, an electromagnetic wave is injected from one terminal of winding, and the power of the wave at the receiving terminal is measured. The power at the terminals is measured in terms of either voltage or current. This difference in power at the two terminals can be attributed to the medium's permittivity, permeability and conductivity, through which the signal is being transmitted. This paper offers an explanation for the behavior of the voltage gain frequency response of induction motor winding and propagating medium parameters by employing the fundamental electromagnetic wave equations. Their explanation illustrates how these parameters can affect the response. The correlation established using Maxwell's equation and these parameters with frequency response analysis is evident while identifying open winding fault and issue with machine core inductance. The results are analyzed and interpreted with the new correlation.*

Keywords

Condition monitoring, Electromagnetic waves, Frequency response analysis, Induction machine diagnosis, Maxwell's equations.

1. Introduction

An electromagnetic wave (Eq. 1) is a physical phenomenon that propagates in both space and time through a medium. These waves transfers energy from one end to another, with or without a conductor. One such example is the transmission line. This electrical energy is consumed globally, supplied via transmission lines and is utilised to power a variety of industries.

$$A(x,t) = A_{max}\cos(k\,x - \omega\,t) \tag{1}$$

Approximately 85% of the industry's electrical machines are induction motors, primarily squirrel cage motors. Their robust structure and ease of control using power electronic converters are the primary reasons for their high demand in low, medium and high power industrial applications [1].

These motors are used in various mechanical applications, such as driving draught pumps in power plants, pumping water to cooling towers, driving conveyor belts, etc.. The absence of the brush & slip-ring arrangement in squirrel cage machines results in spark-free operation; this makes them ideal for use in explosion prone environments, such as the oil industry, petroleum industry, and coal mining, among others [2].

For such important operations, well-conceived maintenance strategy will guarantee a safe and uninterrupted operation in the industry. Maintenance engineers most frequently employ three maintenance strategies viz. *Breakdown maintenance*, *Time-based maintenance* & *Condition-based maintenance*. The maintenance method is selected and implemented based on the machine's size, redundancy, importance to the system and it's financial impact on the industry.

Researchers and scientists have developed condition monitoring techniques to detect mechanical anomalies in an induction motor over the past few decades. These methods compare the effect caused by a specific parameter during normal and abnormal operations to ascertain the nature and cause of a fault [3, 4, 5].

Motor current signature analysis and the vibration analysis are the methods widely studied in the domain of condition monitoring of induction motor as they are non-invasive and online methods. Observing the partial power spectrum of the induction motor [6] and measuring axial emf with a search coil [7] are among a few of the many techniques described in the literature.

Motor current signature analysis monitors the frequency spectrum of stator current for a fully loaded induction motor [8, 9, 10]. The presence of specific frequency components aids in the diagnosis of machine rotor broken bar, bearing, and eccentricity faults.

Vibration sensors attached to the machine's body are used to monitor the mechanical vibrations in the machine [11]. The recorded vibration spectrum is processed via wavelet transform or short-time Fourier transform in order to identify mechanical defects.

The current waveform or vibration in a machine is dependent on a number of other parameters, such as supply voltage, machine design parameters, loading condition, etc. This implies that the presence of fault-detection frequency components in the current signal or vibration signal may result from the aforementioned uncertainties, thereby creating a false impression of a mechanical fault.

This shortcoming of current signature and vibration analysis prompted authors to investigate and implement frequency response-based diagnosis in induction motor.

The frequency response is an offline, non - invasive condition monitoring technique; employed widely to detect mechanical deformations in a transformer [12, 13, 14].Multiple sinusoidal low voltage signals are used to energize the winding at one terminal and the responses to these signals are recorded at another terminal (based on the circuit connections). The principle behind this technique is electrical resonance [15], in which the R, L and C parameters of the winding, leads to the presence of peaks and troughs, based on the connection arrangements used for the measurment.

Frequency response analysis is a comparison-based technique in which the traces are compared to a reference trace, also known as baseline data, which is typically provided by the manufacturer. When baseline data is unavailable, a comparison is conducted between the trace of an identical unit or among the phases of the same unit, assuming the phase winding is congruent. This test is performed to verify the winding's electrical and mechanical integrity after various incidents, such as lightning strikes, seismic events, post-transportation assembly, etc.; used for routine diagnostics, etc. Diagnostics for critical induction motors can also be conducted using an equivalent approach.

The authors here are listing some of the work carried out in the domain of transformer diagnosis using freqeuncy response which the readers can work upon in the case of induction motor diagnosis.

- The comparison of frequency with baseline data can be conducted visually, or with the aid of statistical indicators such as the Arithmetic Sum of Logarithmic error (ASLE), Variance, Min-Max ratio, Compartitive standard deviation (CSD), t-test, Root Mean Square Error (RMSE), and others [16, 17].
- A R-L-C ladder network exhibiting the similar frequency behaviour as the physical system is synthesized and described for driving point impedance connection in [18, 19].
- The frequency response spectrum is divided into small sections, which attributes the faulty component of the transformer by varying the circuit parameters of the R-L-C network of the transformer, which helps to identify the fault component [20].
- The analysis of frequency response in terms of poles and zeros of the transfer function is studied and reported for normal and abnormal transformer conditions [21, 22].
- The behaviour of frequency response due to other factors such as connection cables, terminating resistances, environmental effects, etc. is studied and reported in the literature [23].

The method of FRA is used for the detection of stator winding faults in induction motors [24, 25, 26, 27, 28, 29], also, the effect of winding connection arrangement on the frequency response for the winding fault is demonstrated and studied using various statistical indicators [30]. The frequency response is also, used to determine the *differential-mode*, *common-mode*, and *zero-sequence* impedances of the induction motor to study the effect of shaft voltage and bearing currents in PWM inverter drives. The high-frequency circuit models of induction motor representing the frequency response for the listed impedances is available in [31, 32]. However, these circuits are exclusively used for the study of shaft voltages and bearing currents and are not suitable for the diagnosis, as the frequency response connection arrangements may differ to the measurement connection used for *differential mode*, *common mode* and *zero-sequence impedances*.The influence of rotor position on the frequency response of a rotating machine is discussed in [33].

In this paper, the authors present the voltage gain frequency response of an induction motor winding and propose a novel explanation for the response's behaviour employing the fundamentals of electromagnetic wave propagation.

In the subsequent sections, the authors explained the experimental setup developed in the laboratory and the summary of the experiments carried out; the authors have illustrated and explained the frequency response of an open-turn fault in an induction motor winding using the proposed explanation; in addition, the effect of core inductance on the frequency response of the machine winding is studied, shown and explained using electromagnetic wave equations. The proposed explanation is used to identify and distinguish the open turn fault in the winding apart from the fault introduced due to magnetic core in the machine.

2. Frequency response of Induction machine

2.1. Experimental setup

The frequency response measurement system is developed in the laboratory using an Arbitrary Function Generator (AFG) and a Digital Signal Oscilloscope (DSO) (Tab. 1); both the instruments are programmable and communicated over USB using MATLAB [34, 35].

The AFG is configured to produce sine wave with frequency ranging from 20 Hz to 1 MHz. The study employs a total of 1200 frequency points, logarithmically spaced over frequency range [36]. The voltage sine wave is injected into one of the coil's terminals. The magnitude of the gain is computed by capturing the peak values of the input voltage (V_i) and output voltage (V_o), i.e. $20 * log_{10} \frac{V_o}{V_i}$. In addition, the phase difference of the system is computed by identifying the peak time instant for V_o and V_i. Gain and phase difference are plotted with their respective frequency and the resulting trace represents the frequency response of the coil. The discretization effect and measurement noise are reduced by processing captured waveform with a sine wave curve fitting algorithm [37].

Another method for capturing frequency response is described in [38], which provides only gain-magnitude data. This method of measurement is faster than the system described above.

Tab. 1: Instruments used for frequency response analysis

Instrument	Model Number	Resolution
Arbitrary function generator	Tektronix AFG 3052B	14 - bit
Digital storage oscilloscope	Tektronix TDS 2312	12 - bit

2.2. Connection arrangements

The frequency response of three low-powered induction machines are investigated. The studied machines' stator windings are distributed and randomly wound. The connection configuration for measuring frequency response depends on the accessibility of the winding terminals.

There are two possible connection configurations for measuring the frequency response of an induction motor.

Winding measurement: By injecting the voltage signal at one terminal and observing the output voltage response at the subsequent termination of the winding, the frequency response of the winding is determined. Other windings apart from the test winding are left open (Fig. 1(a)).

Line measurement: In this configuration, the response of series-connected coils is measured. The diagram of the connection is shown in Fig. 1(b). The stator winding contains an inaccessible internal star point.

Machine 1 has an open turn fault in one of the phases, whereas Machines 2 and 3 are used to examine the effect of core inductance on the induction machine frequency response. The specifications of the machine under study is shown in Tab. 2 and the machine's connection configuration and the type of research conducted are detailed in Tab. 3.

Tab. 2: Specifications of the 3 - ϕ induction motors tested

Name	Power	Voltage	Current	Frequency	Power Factor	Speed
Machine 1	5 hp	415 V	7 A	50 Hz	0.745	2800 rpm
Machine 2	5 hp	415 V	7.6 A	50 Hz	0.79	1440 rpm
Machine 3	3 hp	415 V	3.91A	50 Hz	0.8	1440 rpm

2.3. An induction motor's typical frequency response and electromagnetic waves

.

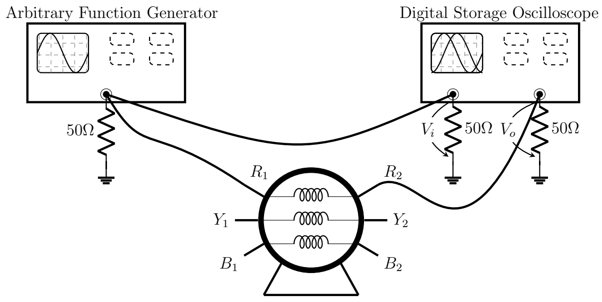

(a) Connection for winding measurement.

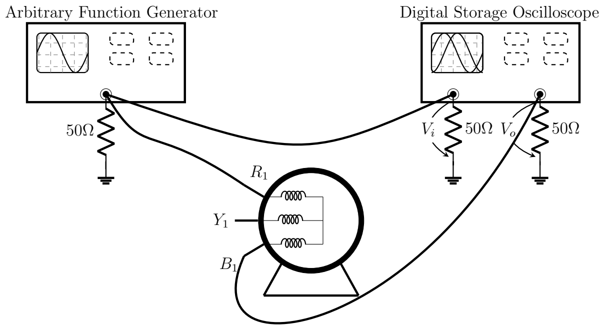

(b) Connection for line measurement.

Fig. 1: Connection arrangement for FRA of induction machine (a) Connection for winding measurement and (b) Connection for line Measurement.

Tab. 3: Summary of experiments.

Machine	Machine Type	Terminal Connections	Connection Arrangement	Type of study
Machine 1	Squirrel cage motor	6 stator terminals (2 per phase)	Winding measurement	Open turn fault
Machine 2	Squirrel cage motor	6 stator terminals (2 per phase)	Winding measurement	Effect of rotor core
Machine 3	Slip ring motor	6 terminals (1 per stator winding and rotor winding)	Line measurement	Effect of magnetic core

The Fig. 2 depicts a typical frequency response of healthy induction motor [27]; due to the presence of one resonance point in the trace (Fig. 2), the trace is divided into two parts , i.e. a segment with $\omega < \omega_r$ and the other segment with $\omega > \omega_r$, where ω_r is the resonating frequency. The response can be further divided into multiple regions, based on the presence of resonance frequencies.

The behaviour observed in the trace (Fig. 2) of the winding can be explained using the transmission line analogy and applying Maxwell's equation for electromagnetic wave propogation (Eq. 2 & Eq. 3).

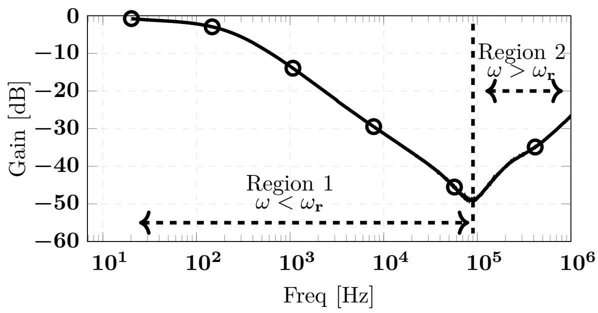

Fig. 2: Typical voltage gain frequency response of induction machine.

$$\nabla \times \mathbf{E} = -j\omega\,\mathbf{B} \tag{2}$$

$$\nabla \times \mathbf{B} = \sigma\,\mu\,\mathbf{E} + j\left(\frac{\omega}{v^2}\right)\mathbf{E} \tag{3}$$

$$\lambda = \frac{v}{f} \tag{4}$$

$$v = \frac{1}{\sqrt{\mu\varepsilon}} \tag{5}$$

$$I_c = \sigma\,\mu\,\mathbf{E} \tag{6}$$

$$I_d = j\left(\frac{\omega}{v^2}\right)\mathbf{E} \tag{7}$$

In a transmission line, the frequency of the wave is the same at both ends, but the velocity (Eq. 5) of the wave as it progresses through a medium varies depending on the medium's *permeability* (μ) and *permittivity* (ε). Consequently, a wave travelling through different mediums will experience a change in wavelength, resulting in a phase difference between the sending end wave and the receiving wave.

The downward slope observed in region 1 ($\omega < \omega_r$) of Fig. 2 is due to the dominant conduction current component (Eq. 3). The (Eq. 6), indicates that the conduction current is independent of the frequency but, the *relative permeability* (μ_r) of a ferromagnetic material is frequency sensitive, as reported in [39]. This study has reported that μ_r is constant up to 1×10^3 Hz and then begins to decline, reaching unity for frequencies greater than 1×10^5 Hz. This decline results in the reduction of conduction current component, resulting in a downward slope in voltage gain of the induction motor. Here, the consequences of skin effect on conductivity of the winding is neglected.

In the region 2 of the frequency spectrum ($\omega > \omega_r$), the displacement current component Eq. 7 dominates, which is dependent on the wave *frequency* (ω) and the medium parameters; *permittivity* (ε) and *permeability* (μ) of the medium. In this range of testing, the medium's *permeability* is now equal to that of vacuum and remains constant. In addition, the *permittivity*(ε) of the medium (insulators) is constant over the test frequency range [40]. Consequently, the velocity of the traversing wave is constant, and the magnitude of the displacement current is frequency-dependent; hence the rise in output voltage V_o, which can be observed as a rising slope in region 2 of frequency response.

2.4. Fault identification

The frequency response of machine 1 is depicted in Fig. 3. Since neither the baseline data nor the sister unit is available, the fault is identified by comparing the frequency response of individual windings. In the low-frequency region, winding $R - R_1$ lacks the initial downward slope, and its output voltage V_o is lower than that of the other windings.

Referring Sec. 2.3. , the conduction current contributes primarily to the output voltage in region 1 of the spectrum. Variation in medium's conductivity (σ) or permeability (μ) may account for the reduced conduction current.

All of the phase windings are wound on a single core, and the presence of a downward slope in the traces of the other two windings indicates that the core is healthy. As the medium's *permeability* (μ) remains unchanged, the *conductivity* (σ) of the conductor must have changed. Since the conduction current decreases, and based on the Eq. 6, we can infer that the *conductivity* (σ) of the medium is reduced, indicating an open winding. A rise in the voltage gain in region 1 of $R-R_1$ trace, is due to the dominant contribution of the displacement current over conduction current component.

A visual examination of the machine revealed that a few turns of the phase R winding have burnt (Fig. 4). Also, the measured resistance values for all the windings are presented in Tab. 4.

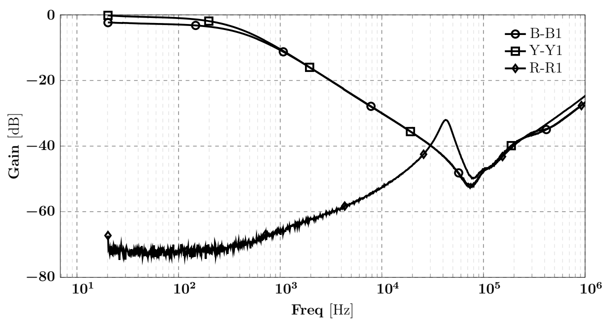

Fig. 3: Frequency response of machine 1.

2.5. Effect of rotor core

In order to examine the effect of the rotor core on the frequency response, the frequency response of machine 2 is measured under two conditions: (i) with the rotor assembly and (ii) without the rotor assembly. Measurement is performed using the winding connection configuration. The frequency response for both cases is illustrated in the Fig. 5. Gain variation is observed among cases in the low-frequency region of the frequency response spectrum, as anticipated.

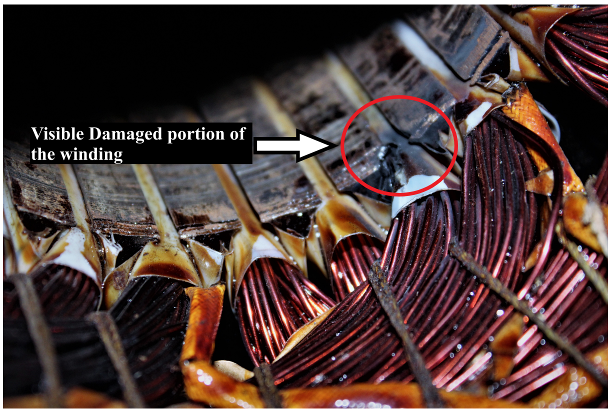

Fig. 4: Photograph of a faulty part in machine 1.

Tab. 4: Measured parameters of winding

Phase	Resistance (Ω)
R - phase	121
Y - phase	4.1
B - phase	18

In case (i) the medium permeability μ_{med1} is the result of all three cores, i.e., stator core (μ_{st}), air-gap(μ_{ag}) & rotor core (μ_{rt}), whereas in case (ii), the medium permeability μ_{med2} is the result of μ_{st} & μ_{ag}.

As, the traversing medium involving the rotor has a greater permeability ($\mu_{\mathrm{med1}} > \mu_{\mathrm{med2}}$), lower current is required to generate the same amount of flux, compared to case (ii). Hence, the lesser output voltage V_o. This anomaly is observed in the Fig. 5, wherein the response for case (i) is lower compared to case (ii).

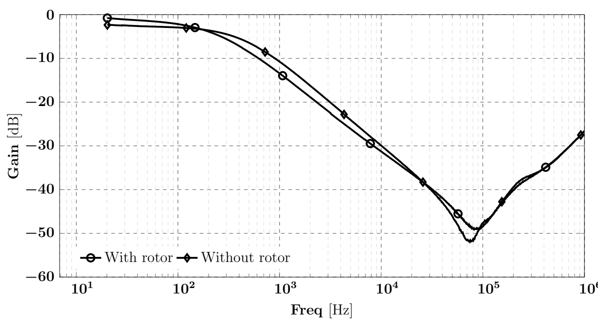

Fig. 5: Effect of core inductance on frequency response of machine 2.

For the high-frequency region, the traces are identical in both cases. As discussed previously, medium permeability is $\mu_{\mathrm{med1}} = \mu_{\mathrm{med2}} = \mu_0$. In addition, ε is constant; consequently, the wave velocity for a given frequency is identical for both cases, making the responses identical.

To confirm the same, a similar study is conducted on machine 3, which is a slip-ring machine. In this study, the frequency response of both the stator and the rotor is measured via the line connection. The frequency response of the stator (or rotor) winding is measured with the following conditions: (i) rotor (or stator) terminals kept open, and (ii) rotor (or stator) terminals shorted. The connection configurations are depicted in Fig. 6.

The frequency response for the stator winding is depicted in Fig. 7(a), while the frequency response for the rotor winding is depicted in Fig. 7(b). The results demonstrate the similar behaviour mentioned in the earlier paragraph.

3. Conclusion

The frequency response for an induction motor winding is presented and analyzed with a novel approach to distinguish and identify the winding fault(s). A very different approach to study the frequency response of induction machine winding using concepts of electromagnetic wave propagation equations is adopted. This way suggests that the conduction current drawn by the circuit is responsible for variation in low frequency region of the frequency response, leading to highlighting an open turn fault in the machine winding. This approach offered an explanation to the deviation in frequency response due to core inductance variation and hence established relationship with the conduction current.

The high frequency region in the responses indicated a match. The physics of wave propagation supported it due to the fact that displacement current remains unchanged; as the medium parameters are constant in this frequency range, resulting in a constant wave velocity.

The experimental results presented through cases in this research work indicates that frequency response analysis can be extended well as a diagnostic tool for the three phase induction motor and the electromagnetic wave propagation effectively helps fault identification and interpretations.

Author Contributions

H.A. was responsible for developing the measurement system and carrying out the experiments. He put out a theory to explain the varying findings that were discovered when the experiment was conducted in a variety of settings. S. V. was in charge of supervising the tests, as well as contributing to the documentation of them and revising the draft paper. K. B. was in charge of overseeing the tests and provided input throughout the paper review.

References

[1] KUMAR S., D. MUKHERJEE, P. GUCCHAIT, R. BANERJEE, A. SRIVASTAVA, D. VISHWAKARMA and R. SAKET. A comprehensive review of condition based prognostic maintenance (cbpm) for induction motor. *IEEE Access*. 2019, vol. 7, pp. 90690–90704. DOI: 10.1109/ACCESS.2019.2926527.

[2] THORSEN O. and M. DALVA. A survey of faults on induction motors in offshore oil industry, petrochemical industry, gas terminals, and oil refineries. *IEEE Transactions on Industry Applications*. 1995, vol. 31, iss. 5, pp. 1186–1196. ISSN 0093-9994. DOI: 10.1109/28.464536.

[3] NANDI S., H. TOLIYAT, and X. LI. Condition monitoring and fault diagnosis of electrical motors—a review. *IEEE Transactions on Energy Conversion*. 2005, vol. 20, iss. 4, pp. 719–729. ISSN 0885-8969. DOI: 10.1109/TEC.2005.847955.

[4] TAVNER P. Review of condition monitoring of rotating electrical machines. *IET Electric Power Applications*, 2008, vol. 2, iss. 4, pp. 215–247(32). ISSN 1751-8660. DOI: 10.1049/iet-epa_20070280.

[5] BINDU S. and V. THOMAS. Diagnoses of internal faults of three phase squirrel cage induction motor — a review. *2014 International Conference on Advances in Energy Conversion Technologies (ICAECT)*. 2014, pp. 48–54. DOI: 10.1109/ICAECT.2014.6757060.

[6] TRZYNADLOWSKI M. Detection of mechanical abnormalities in induction motors by electric measurements. *International Journal of Rotating Machinery*. 1999, vol. 5 , iss. 1, pp. 41–52. ISSN 1023-621X. DOI: 10.1155/S1023621X99000044.

[7] PENMAN J., H. SEDDING, B. LLOYD, and W. FINK. Detection and location of interturn short circuits in the stator windings of operating motors. *IEEE Transactions on Energy Conversion*. 1994, vol. 9, iss. 4, pp. 652–658. ISSN 0885-8969. DOI: 10.1109/60.368345.

[8] FILIPPETTI F., G. FRANCESCHINI, C. TASSONI, and P. VAS. AI techniques in induction

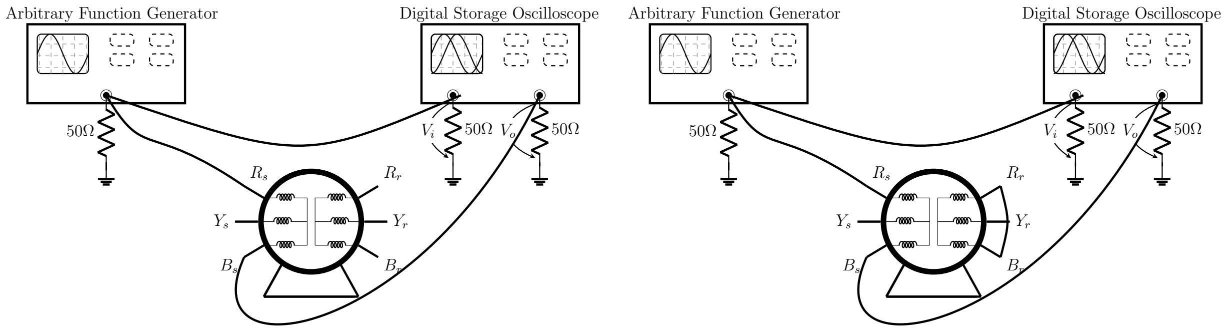

(a) Stator winding frequency response (rotor terminal open). (b) Stator winding frequency response (rotor terminal short).

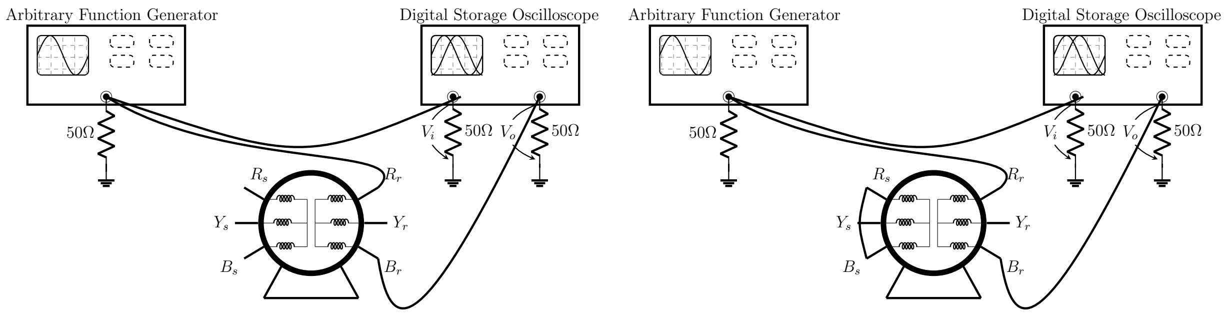

(c) Rotor winding frequency response (stator terminal open). (d) Rotor winding frequency response (stator terminal short).

Fig. 6: Connection arrangement for FRA of induction machine (a) Stator winding frequency response (rotor terminal open), (b) Stator winding frequency response (rotor terminal short), (c) Rotor winding frequency response (stator terminal open) and (d)Rotor winding frequency response (stator terminal short).

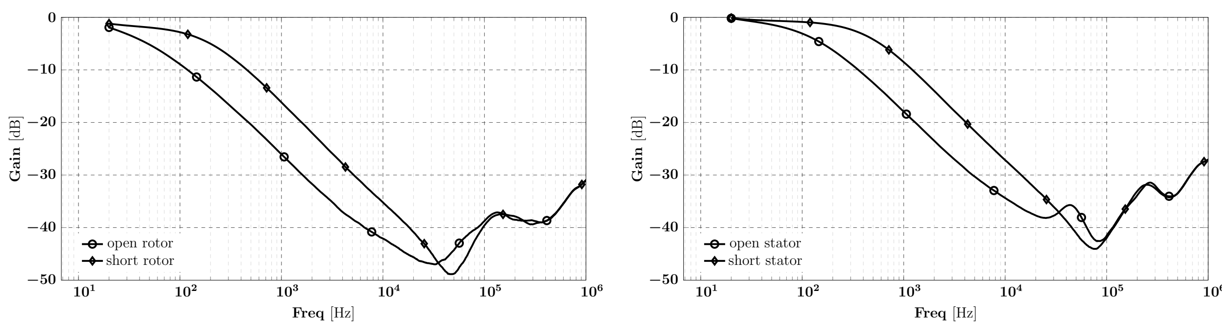

(a) Frequency response of machine 3 (stator side). (b) Frequency response of machine 3 (rotor side).

Fig. 7: Connection arrangement for FRA of induction machine (a) Frequency response of machine 3 (stator side) and (b) Frequency response of machine 3 (rotor side).

machines diagnosis including the speed ripple effect. *IEEE Transactions on Industry Applications.* 1998, vol 3, iss. 1, pp. 98–108. ISSN 0093-9994. DOI: 10.1109/28.658729.

[9] BELLINI A., C. CONCARI, G. FRANCESCHINI, E. LORENZANI, C. TASSONI, and A. TOSCANI. Thorough understanding and experimental validation of current sideband components in induction machines rotor monitoring. *IECON 2006 - 32nd Annual Conference on IEEE Industrial Electronics.* 2006, pp. 4957–4962. DOI: 10.1109/IECON.2006.347586.

[10] KLIMAN G., R. KOEGL, J. STEIN, R. ENDICOTT, and M. MADDEN. Non- invasive detection of broken rotor bars in operating induction motors. *IEEE Transactions on Energy Conversion*, 1988, vol. 3, iss. 4, pp. 873–879. ISSN 0885-8969. DOI: 10.1109/60.9364.

[11] TSYPKIN M. Induction motor condition monitoring: Vibration analysis technique - a practical implementation. *2011 IEEE International Electric Machines & Drives Conference (IEMDC)*, 2011, pp. 406–411. ISBN 978-1-4577-0060-6. DOI: 10.1109/IEMDC.2011.5994629.

[12] ABU-SIADA A. , N. HASHEMNIA, S. ISLAM, and MOHAMMAD A.S. MASOUM. Understanding power transformer frequency response analysis signatures. *IEEE Electrical Insulation Magazine.* 2013, vol. 29, iss. 3, pp. 48–56. ISSN 0883-7554. DOI: 10.1109/MEI.2013.6507414.

[13] CHAKRAVORTI S., D. DEY, and B. CHATTERJEE. *Recent Trends in the Condition Monitoring of Transformers.* London: Springer London, 2013. ISBN 978-1-4471-5549-2.

[14] PICHER P., S. TENBOHLEN, M. LACHMAN, A. SCARDAZZI, and P. PATEL. Current state of transformer fra interpretation: On behalf of cigre WG A2.53. *Procedia Engineering.* 2017, vol. 202, pp. 3–12. ISSN 1877-7058. DOI: 10.1016/j.proeng.2017.09.689.

[15] PRAMANIK S. and L. SATISH. A critical review of the definition of FRA resonance frequency of transformers as per IEEE std C57.149-2012. *Electric Power Systems Research.* 2015, vol. 121, pp. 52–57. ISSN 0378-7796. DOI: 10.1016/j.epsr.2014.11.027.

[16] BEHJAT V. and M. MAHVI. Statistical approach for interpretation of power transformers frequency response analysis results. *IET Science, Measurement & Technology.* 2015, vol. 9, iss. 3, pp. 367–375. ISSN 1751-8830. DOI: 10.1049/iet-smt.2014.0097.

[17] BADGUJAR K., M MAOYAFIKUDDIN, and S V KULKARNI. Alternative statistical techniques for aiding SFRA diagnostics in transformers. *IET Generation, Transmission & Distribution.* 2012, vol. 6, iss. 3, pp. 189–198. ISSN 1751-8687. DOI: 10.1049/iet-gtd.2011.0268.

[18] MUKHERJEE P. and L. SATISH. Construction of Equivalent Circuit of a Single and Isolated Transformer Winding From FRA Data Using the ABC Algorithm. *IEEE Transactions on Power Delivery.* 2012, vol. 27, iss. 2, pp. 963–970. ISSN 0885-8977. DOI: 10.1109/TPWRD.2011.2176966.

[19] MUKHERJEE P. and L. SATISH. Construction of equivalent circuit of a transformer winding from driving-point impedance function – analytical approach. *IET Electric Power Applications.* 2012, vol. 6, iss. 3, pp. 172–180. ISSN 1751-8660. DOI: 10.1049/iet-epa.2011.0150.

[20] ABEYWICKRAMA N., Y. SERDYUK, and S. GUBANSKI. Effect of core magnetization on frequency response analysis (FRA) of power transformers. *IEEE Transactions on Power Delivery.* 2008, vol. 23, iss. 3, pp. 1432–1438. ISSN 0885-8977. DOI: 10.1109/TPWRD.2007.909032.

[21] SATISH L. and A. JAIN. Structure of transfer function of transformers with special reference to interleaved windings. *IEEE Transactions on Power Delivery.* 2002, vol. 17, iss. 3, pp. 754–760. ISSN 0885-8977. DOI: 10.1109/TPWRD.2002.1022800.

[22] NARAYANA G., K. BADGUJAR, and S. V. KULKARNI. Factorisation-based transfer function estimation technique for deformation diagnostics of windings in transformers. *IET Electric Power Applications.* 2013, vol. 7, iss. 1, pp. 39–46. ISSN 1751-8660. DOI: 10.1049/iet-epa.2012.0148.

[23] SAMIMI M., S. TENBOHLEN, A. AKMAL, and H. MOHSENI. Dismissing uncertainties in the FRA interpretation. *IEEE Transactions on Power Delivery.*2018, vol. 33, iss. 4, pp. :2041–2043. ISSN 0885-8977. DOI: 10.1109/TPWRD.2016.2618601.

[24] BRANDT M. and S. KAŁčÁK. Failure identification of induction motor using SFRA method *2016 ELEKTRO.* 2016, pp. 269–272. ISBN 978-1-4673-8698-2. DOI: 10.1109/ELEKTRO.2016.7512079.

[25] VILHEKAR T., M. BALLAL, and B. UMRE. Application of sweep frequency response analysis for the detection of winding faults in induction motor. *IECON 2016 - 42nd Annual Conference of the IEEE Industrial Electronics Society.* 2016, pp. 1458–1463. ISBN 978-1-5090-3474-1. DOI: 10.1109/IECON.2016.7793565.

[26] CIANCETTA F., A. PIZZO, C. OLIVIERI, N. ROTONDALE, L. CASTELLINI, and M. D'ANDREA. SFRA technique applied to fault diagnosis on stators of electric motors. *2014 International Symposium on Power Electronics, Electrical Drives, Automation and Motion*. Italy: IEEE, 2014, pp. 515–520. ISBN 978-1-4799-4749-2. DOI: 10.1109/SPEEDAM.2014.6871937.

[27] AL-AMERI S., A. ALAWADY, M. YOUSOF, M. KAMARUDIN, A. SALEM, A. ABU-SIADA, and M. MOSAAD. Application of frequency response analysis method to detect short-circuit faults in three-phase induction motors. *Applied Sciences*,2022, vol. 12, iss. 4. DOI: 10.3390/app12042046.

[28] BUCCI G., F. CIANCETTA, and E. FIORUCCI. Apparatus for Online Continuous Diagnosis of Induction Motors Based on the SFRA Technique. *IEEE Transactions on Instrumentation and Measurement*.2020, vol. 69, iss. 7, pp. 4134–4144. ISSN 0018-9456. DOI: 10.1109/TIM.2019.2942172.

[29] A. A. ALAWADY, M. F. M. YOUSOF, N. AZIS, and M. A. TALIB. Frequency response analysis technique for induction motor short circuit faults detection. *International Journal of Power Electronics and Drive Systems (IJPEDS)*, 11(3):1653, sep 2020. DOI: 10.11591/ijpeds.v11.i3.pp1653-1659.

[30] SALEM MGAMMAL AL-AMERI, ZULKURNAIN ABDUL-MALEK, *et al.* Frequency response analysis for three-phase star and delta induction motors: Pattern recognition and fault analysis using statistical indicators. *Machines*, 11(1):106, jan 2023. DOI: 10.3390/machines11010106

[31] ION BOLDEA. Super-high-frequency models and behaviour of IMs. In *Induction Machines Handbook*, pages 79–97. CRC Press, may 2020. DOI: 10.1201/9781003033424-3

[32] MIRAFZAL B., G. SKIBINSKI, R. TALLAM, D. SCHLEGEL, and R. LUKASZEWSKI. Universal induction motor model with low-to-high frequency-response characteristics. *IEEE Transactions on Industry Applications*. 2007, vol. 43, iss. 5, pp. 1233–1246. ISSN 0093-9994. DOI: 10.1109/TIA.2007.904401.

[33] SANT'ANA W., G. TORRES AND L. DA SILVA AND E. BONALDI AND L. DE OLIVEIRA AND C. SALOMON and J. DA SILVA, Influence of rotor position on the repeatability of frequency response analysis measurements on rotating machines and a statistical approach for more meaningful diagnostics. *Electric Power Systems Research*, 2016, vol. 133, pp. 71–78. ISSN 0378-7796. DOI: 10.1016/j.epsr.2015.11.044.

[34] Tektronix. *Programmer manual: AFG3000 Series Arbitrary / Function Generators 071-1639-04*. 2015. Available at: `https://www.tek.com/en/function-generator/afg3000-function-generator-manual/afg3000-series`

[35] Tetronix. *TDS2000 Series Digital Oscilloscopes: Programmer Manual*. 2006. Available at: `https://www.tek.com/en/oscilloscope/tds210-manual/tds200-tds1000-tds2000-tds1000b-\tds2000b-and-tps2000-programmer`.

[36] IEEE std. C57.149-2012. *IEEE Guide for the Application and Interpretation of Frequency Response Analysis for Oil Immersed Transformers*. IEEE, 2013.

[37] IEEE Std 1057-2017 (Revision of IEEE Std 1057-2007). *IEEE standard for digitizing waveform recorders*. IEEE, 2018.

[38] SATISH L. and S. VORA. Amplitude frequency response measurement: A simple technique. *IEEE Transactions on Education*. 2009, vol. 53, iss. 3, pp. 365–371. ISSN 0018-9359. DOI: 10.1109/TE.2009.2023082.

[39] TRELA K. and K. GAWRYLCZYK. Frequency response modeling of power transformer windings considering the attributes of ferromagnetic core. *2018 International Interdisciplinary PhD Workshop (IIPhDW)*. Poland: IEEE, 2018, pp. 71–73. ISBN 978-1-5386-6143-7. DOI: 10.1109/IIPHDW.2018.8388328.

[40] KASAP S. *Principles of electrical engineering materials and devices*. Boston: Irwin McGraw-Hill, Mass., 1997. ISBN 978-0256161731.

About Authors

Hormaz AMROLIA (corresponding author) Hormaz Amrolia was born in 1989. He received B.E. in electrical engineering from ADIT, V. V. Nagar, Gujarat, India in 2010 and completed M.Tech in power electronics, machines and drives in 2012 from Nirma University, Ahmedabad, Gujarat, India. He is currently a research scholar in Gujarat Technological University, India. His major field of studies are power electronics and electrical machines. He is currently working as an assistant Professor in electrical department, Nirma University, Ahmedabad, Gujarat, India. His research area is electrical machine diagnostics.

Santosh VORA was born in 1974. He received the B.E. degree in electrical engineering from Saurashtra University, Rajkot, India, in 1997 and the M.E. and Ph.D. degree in Electrical Engineering with specialization in High-Voltage engineering from the Indian Institute of Science (IISc), Bangalore, in 2004 and 2009 respectively. At present, he is working as Professor in the Dept. of Electrical Engineering, Institute of Technology, Nirma University, Ahmedabad. His research areas include power system dynamics, effect of inclusion of renewable systems in the conventional power system, permanent magnet machines and high-voltage measurement related instrumentation and diagnostics.

Ketan BADGUJAR was born in the city of Ahmedabad in the year of 1975. He received his B.E. in electrical engineering in the year of 1997 from L.D.C.E, Ahmedabad, Gujarat, India. He received M.E. in high voltage engineering from IISC, Bangalore, Karnataka, India in the year of 2007 and completed his Ph.D from IIT Bombay, Maharashtra, India in the year of 2013. His major field of studies are Electrical engineering and High voltage engineering. He is having an experience of 25 years in the field of teaching and currently he is Professor in electrical department S.S.E.C, Bhavnagar. His area of research is diagnosis of electrical machines.